

A Vortex Plate Theory of Hovering Animal Flight

Khaled. M. Faqih

Abstract—A model of vortex wake is suggested to determine the induced power during animal hovering flight. The wake is modeled by a series of equi-spaced rigid rectangular vortex plates, positioned horizontally and moving vertically downwards with identical speeds; each plate is generated during powering of the functionally wing stroke. The vortex representation of the wake considered in the current theory allows a considerable loss of momentum to occur. The current approach accords well with the nature of the wingbeat since it considers the unsteadiness in the wake as an important fluid dynamical characteristic. Induced power in hovering is calculated as the aerodynamic power required to generate the vortex wake system. Specific mean induced power to mean wing tip velocity ratio is determined by solely the normal spacing parameter (f) for a given wing stroke amplitude. The current theory gives much higher specific induced power estimate than anticipated by classical methods.

Keywords—vortex theory, hovering flight, induced power, Prandtl's tip theory.

I. INTRODUCTION

HOVERING phenomenon is aerodynamically an extreme mode of flying that necessitates a tremendous energy expenditure since all downward movement of air requisite to neutralize the effect of gravity on the hovering animal for the duration of the wing beat must be supplied by the beating wings. The mechanical power input is expected to be unobtainable especially for animals which are not characteristically suited to utilize hovering flight as a locomotion means during their life cycle since their power budget can not tolerate such massive amount of power consumption. The flow field produced during hovering animal flight is extraordinarily difficult to treat mathematically and the associated wing kinematics is of great complexity to perceive. The resulting flow pattern is periodically-generated nearly equally spaced twisted vortex sheets. The complexity of this flow requires a more elaborate modeling of its structure to obtain an accurate computation of the induced velocity developed at the wing disk. Numerical methods are the outcome of most flight models and the accompanying computing time is normally astronomical. However, the vortex lattice illustration of the wake utilized in present theory is computationally the most economical.

Early quantitative approaches introduced drastic simplifications to the wake structure such as neglecting the

unsteadiness of the wake by assuming that vorticity is distributed throughout the wake volume rather than in a discrete pattern. These methods can only describe the general airflow characteristic and it does not require any detailed knowledge of the internal process within the fluid. Most of the early studies on hovering flight adopted the actuator disk and its associated momentum jet. These methods assume that the flapping motion imparts continuous momentum to the air, and the lift force is generated as a result of accelerating the air vertically downwards. The momentum jet theory assumes that no flow passes through the boundary of the wake, and that both mass and momentum are conserved in the body of the wake. The classical methods are elegant in their simplicities and can reduce the complexity of the mathematical treatment enormously. In fact, animal flight produces a very complex wake structure which sequentially generates a highly complicated airflow pattern over the wings and around the resulting vortex sheets. Also the vorticity generation during hovering activity is discontinuous, consequently there can be a flow through the boundary of the wake which violates strongly the continuity requirement assumed by the conventional aerodynamic analysis. The validity of these assumptions in application to animal flight is therefore limited. Apparently these discrepancies can not be disregarded and should be sufficiently adequate to dispense with the utilizing of momentum jet theory in animal flight analysis [1], [2], [3], [4], [5].

The blade element theory of propellers has been widely used to study the animal flight. This theory assumes that the wing is operating under quasi-steady aerofoil states. The aerodynamic effects of wing motion are calculated by assuming that the aerodynamic forces produced by each element of the wing are identical to those that would be produced by such element traveling at the same steady velocity and angle of attack. [6] derived the general equations that apply to flapping flight. This type of analysis nevertheless requires a knowledge of lift and drag coefficients. The classical studies of flapping flight composed of a blade element theory which provides the lift and drag forces and a momentum theory that gives the induced velocity at the wing disk [7], [8], [9], [10]. Theoretical and experimental predictions for the force coefficients contain numerous 'gray areas' of uncertainty which force the employment of a number of simplifying assumptions to obtain approximate estimates to them. It is evident that conventional aerodynamic analysis is incapable of providing a detailed knowledge of the flow field and can not fully tackle the animal flight problem. However,

Khaled M. S. Faqih is with the Information Systems Department, Al al-Bayt University, Jordan (e-mail: km_faqih@aabu.edu.jo).

the final equations resulted from the current vortex plate theory are independent of the lift and drag coefficients.

A high degree of unsteadiness in the flow necessitates an aerodynamic modeling that based on a consideration of the local flow characteristic rather than on a global properties as in the case of classical methods. [11] was the first to put forward a flight vortex theory. He set up the general equations for his flight theory, but they were too complex to manage mathematically. [12] developed a vortex hovering theory; he suggested that the vortex sheet shed by the powered stroke rolled up immediately into circular vortex rings. [13] devised a new model based on what he called the pulsed actuator disc, his theory has proved useful for animals that characterize by low wake spacing. Exploiting the recent advances in near-flow aerodynamics of insects and birds, [14] developed a theoretical framework to calculate the mean induced flow and how wing kinematics affects induced flow over flying animals body. This work [14] is derived from rotary aerodynamics. These aerodynamic theories also make use of various assumptions and simplifications to make them mathematically solvable. Nevertheless, flying animals have a sophisticated type of wing design; it is capable of flapping and twisting simultaneously and able to respond to the inertial and aerodynamic forces normally encountered during flight, it also allows changes of velocities and angles. Such complexity has so far hampered any precise modeling of this complex aerodynamic phenomenon.

The theory presented here is designed to model the wake structure of a hovering animal flight. Fundamentally, this type of mathematical modeling presents difficulties in computation and fairly realistic approximations are therefore imperative. This theory is therefore based upon a number of assumptions which reduce the structural and mathematical complexities of the wake and make it qualitatively and quantitatively manageable. The modeling of the wake to be considered in the present theory is the classical rigid wake model; this model assumes no distortion should take place to the geometry of the wake and all the wake elements are convected with the same velocity. The present flight theory retains qualitatively the surface traced out by the flapping wings during the feathering of the aerodynamically loaded stroke as the vortex wake shape under consideration. The twist of the vortex sheets are to be ignored and assumed rectangular. Thus the wake under physical deliberation consists of a chain of equi-spaced rigid impermeable rectangular vortex plates positioned in a horizontal plane in the flowfield and array vertically downwards beneath the wing disk. The vertical wake spacing is decided by the rate at which the vortex plates are convected downwards. However, limits on the accuracy of the solution are imposed by the hypothesis that the wake is not permitted to curl up under the action of local velocities. This paper provides primarily an estimate of mean induced power consumed during hovering action.

II. ASSUMPTIONS, DEFINITIONS AND HOVERING KINEMATIC PATTERNS

The formation of a pragmatically accurate and

mathematically solvable hovering flight model does not rely upon a particularly rigid adherence to the exact geometry of the vortex sheet. Thus simplifying assumptions are introduced to conduct the analysis without unduly lengthy or complex computations. Throughout it is assumed that the fluid is incompressible, inviscid, and of uniform density. This study neglects all viscous lag effects and the azimuthal variation of the vorticity. The deforming effects induced by the presence of vorticity elsewhere in the flow field on the vortex plate under investigation are small enough to be neglected. The rotation which may occur due to the interaction between successive vortex plates in the wake is ignored; normally a newly generated vortex plate causes its predecessor to rotate. The movement of the wing during the functional stroke is assumed to be confined to a single plane and the resulting vortex sheet is characteristically planar. However, departure from planarity may cause a small increase in vortex plate energy, but such increase has little effect on the outcome of the theory and can be ignored. At the commencement of a wing motion, a full establishment of steady-state vorticity production is normally delayed by what so-called the 'Wagner effect'. The interaction between the bound vorticity and the trailed vorticity is merely responsible for this aerodynamically unfavorable state. However, the twist of an animal wing may be assumed such that the effect of Wagner in delaying the lift development, is counterbalanced by pushing the wings to high angle of attack at the start of the downstroke and reducing the incidence throughout the stroke, particularly for hovering birds. The present theory assumes that the undesirable phenomenon of Wagner has a diminishing influence on the progress of the hovering process and can be ignored without introducing any serious errors in the calculation. The present study also neglects totally the roll-up of the vortex wake that may occur downstream of the wing disk since it has little influence on the animal itself and it takes place well downstream about 13 chord lengths behind the wing disk [15]. Also, rolling-up phenomenon should by no means affect the induced power consumption considerably because induced power is little influenced by the exact state of the vortex sheet. Finally, we assume that the interactions among vortex elements under physical deliberation are minimal.

There are two categories of flight parameters associated with the animal features and the generated wake. The first category can be divided into two distinguished groups: the morphology and kinematics groups. The morphological parameters describe the structural features of the animal body and wing; those are the body mass M_b , and wing semi-span b . The kinematic parameters feature the wing stroke dynamical characteristics; they are the stroke plane angle of the wing relative to the horizontal β , stroke amplitude ($2\Psi_m$), and the wing stroke period T .

$$\omega_i = \frac{\pi b}{\hat{T}T}, \quad (1)$$

where \hat{T} , is the non-dimensionalized stroke period. It is equal to 1/2 if both half strokes generates lift and 1 if only

downstroke does so. The induced velocity of the vortex plate far downstream of the wing ω_s will be derived later from the consideration of the vortex sheet impulse. By the above definition, normal spacing parameter,

$$f = \frac{\omega_t}{\omega_s}, \quad (2)$$

so that

$$f = \frac{\pi b}{\hat{T}T\omega_s}. \quad (3)$$

We define another important non-dimensional parameter called the hovering parameter K as the square of the ratio between the ideal induced velocity ω_j and wing tip velocity.

The ideal induced velocity can be derived from the actuator disc concept [16], therefore

$$\omega_j = \left[\frac{M_b g}{4\rho\Psi_m b^2} \right]^{1/2}, \quad (4)$$

where ρ ($=1.225 \text{ kg/m}^3$) is the air density. From the above definition, hovering parameter

$$K = \frac{\omega_j^2}{\omega_t^2}. \quad (5)$$

Thus we can write

$$K = \frac{\hat{T}^2 T^2 M_b g}{4\pi^2 \Psi_m \rho b^4}. \quad (6)$$

It is unequivocally apparent that a comprehension of the wing's kinematics during hovering is of paramount consequence in the progression of any vortex flight theory because each kinematic pattern necessitates theoretically somehow different physical deliberations from the others. Great advancements have been made recently concerning the kinematics of the wing motion during hovering [13]. Three main functional patterns have been observed in the field as well as in the laboratory. The categorization of each pattern is based on the orientation of the stroke plane, each kinematic pattern is distinguished by the inclination of its stroke plane.

The first pattern is the most commonly observed kinematic pattern among insects and hummingbirds. It is characterized by a roughly horizontal stroke plane, almost vertically oriented body, figure-of-eight wing movement, and symmetrical down- and up-strokes wing movement. This elegant form of hovering requires peculiar wings' structural anatomy as they need to rotate their wings quickly at the ends of each half-stroke so that they get oriented for the coming stroke, and so the fore edge is always leading; therefore upward-acting forces arise in both half-strokes. This pattern was firstly identified by [10] which he called normal hovering. In his elementary survey, Weis-Fogh employed very simplistic approach based on a steady-state aerodynamic principles and a number of simplifying assumptions to

analytically study this common form of hovering. He calculated the mean lift coefficients and found that most insects are operating within the capabilities of low Reynolds number aerofoils, with the exception of the chalcid wasp, *Encarsia formosa*, its estimated lift coefficient was rather much too high to be compatible with quasi-steady aerodynamics. Later, [13] carried out more accurate estimates of lift coefficient of two insects, a ladybird, *Coccinella 7-punctata*, and a crane fly, *Tipula obsoleta*, his lift coefficient estimates were strikingly too large to be developed by the classical lift generation mechanism. [10] put forward a novel mechanism called 'clap and fling' that explains how the chalcid wasp supports its weight during hovering. In addition, such mechanism significantly enhances the initial circulation generation on the wing so that the discrepancy allied with the Wagner effect can be reduced to some extent. [17] provided a theoretical analysis that advocated this mechanism.

The second kinematic pattern is common among some small hoverflies, birds, bats, and some dragonflies. It is characterized by an oblique stroke plane. In this hovering form, the upstroke is feathered with little vorticity being generated, they achieve this by flexing the wing in a complex manner to zero angle of attack so as to minimize the fluid resistance during the upstroke. The downstroke generates all the necessary vorticity to maintain the hovering body mass airborne at a fixed point in space for the duration of the entire stroke period. The animals typified by this strenuous mode of hovering are incapable anatomically of exploiting the less power-demanding mode that referred to above. In the analysis of this flight mode we disregard all vorticity produced during upstroke, this is justified by their relatively small values.

The final kinematic pattern was originally unveiled by [13] and found out that butterflies utilize uniquely a vertical stroke plane during hovering cycle. On the downstroke the wing is held perpendicular to the direction of its movement, but the upstroke is feathered so that it is parallel to the direction of movement. As far as I am aware, there is no detailed analysis of the vertically oriented hovering mode in the literature. Therefore we will not investigate this kinematic pattern in our study.

III. INDUCED POWER

The majority of theoretical studies in animal flight mechanics have primarily concentrated energy consumption determination. Studies related to power characteristics calculation and measurement are plagued by theoretical and experimental complexities. Most aerodynamic theories have had the tendency to simplify the complex physics of the airflow in the vicinity of the flapping wings and the wake generated behind the flapping wings, so that a mathematically tractable model could be established.

For a hovering flight activity to be sustained energy has to be produced and transferred to the fluid to increase its momentum, so a force impulse (lift reaction) is produced to support the animal's weight. The power requisite to generate this rise in kinetic energy is termed as the induced power.

Induced power can be thought of as an energy-loss due to vortex shedding in the wake, it is equivalent to the mechanical power needed to generate the vortex wake system.

The source of flapping power is the flight muscles. This power is normally produced by the mechanical movement of the flapping wings, the available amount of power is dependent upon the mass of the animal's muscles [18]. Power demand during hovering is extremely high because the power essential to maintain the wings flapping to produce the necessary wake system is generated exclusively by the beating wings, and a considerable amount of this energy is lost due to the tip effects which is associated with the nature of wake dynamical structure of the animal flight. [19] constructed an attractive theoretical model that deals with flight muscle performance, they have estimated that mechanical power

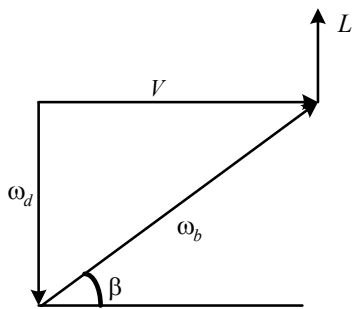


Fig. 1. Diagram of the velocity triangle. ω_d is the induced velocity generated at the wing disk, ω_b is the flapping velocity, V is the resultant velocity, β is the plane stroke angle, and L is the lift generated during hovering action.

output for all kind of flight muscles ranges between 80 and 100 W kg⁻¹. Only a few small birds are able to sustain hovering continuously without incurring an oxygen debt, however, most insects can sustain continuous hovering for long period of times because they produce useful aerodynamic functions during both downstroke and upstroke; they can do so since they are able to spin their wings quickly at the ends of each half-stroke in such a manner that they get oriented for the coming stroke, this extraordinary action is achieved by reversing the upper and lower surfaces through rotating the wings about their longitudinal axis by over 90 degrees between half-strokes. This structural ability is aerodynamically advantageous to insects as well as hummingbirds because they are able to utilize usefully both half-strokes to obtain aerodynamic uplift, unlike most birds which are structurally incapable of performing such action. However, both insects and hummingbirds possess a metabolism system powerful enough to support this extraordinary action of wing movements for long duration.

Many scientists have estimated the power requirements during hovering on the basis of the steady-state ideal principles of actuator disk. [12] has departed from the existing ideal methods and adopted a new approach based on more realistic modeling of vortex wake structure. His estimates

have clearly shown early methods significantly underestimate the induced power requirement. We define the induced power as the power needed to generate the vortex wake system and can be regarded as the power required to neutralize the effect of gravity on the body weight. The mean induced power is estimated (Fig. 1.) as

$$\overline{P}_i = \overline{L\omega_b \sin \beta}, \quad (7)$$

where L is the lift generated during hovering action, this quantity is constant and equals the animal's weight ($M_b g$), and ω_b is the wing flapping velocity. From the velocity triangle (Fig. 1.) it is obvious that

$$\omega_b \sin \beta = \omega_d, \quad (8)$$

where ω_d is the induced velocity at the wing plane. Using equations (7) and (8), we find that

$$\overline{P}_i^* = \overline{\omega_d}, \quad (9)$$

where $\overline{P}_i^* (= \overline{P}_i / M_b g)$ is the specific mean induced power. It is manifested from equation (9) that the specific mean induced power equals the mean induced velocity at the wing plane. The main challenge of the present vortex-plate model is to evaluate the mean induced velocity generated at the wing disk due to the combined aerodynamic effects of the bound circulation and the remainder of the vortex wake.

IV. THE VORTEX WAKE

The most difficult aerodynamical challenge normally encountered when studying animal flapping flight phenomenon is the description qualitatively or quantitatively a realistic presentation of the resulting vortex wake structure. Such wake description may allow a straightforward calculation of induced velocity at the wing disk. This theory is an attempt to propose a realistic vortex model for the wake structure by retaining the surface traced out by the beating wings during hovering as the vortex geometry under consideration because aerodynamic analysis strongly suggests that the geometry of the wake in the vicinity of the wing plane has much greater influence on the animal's aerodynamics than the vortex sheet downstream of the wing, despite to whatever shape the vortex sheet may transform into along its journey. The contraction process will also be regarded as an important phenomenon in the mathematical modeling of hovering flight. We therefore are in no need to make the sweeping assumption that the wake is fully rolled-up in the neighborhood of the wings. Admittedly, many experimental observations explicitly reveal that the behavior of a trailing vortex sheet behind a lifting wing experience the inescapable basic process of rolling-up primarily under the influence of the velocity it induces on itself, besides this phenomenon involves a downstream length scale of an order of four wing spans for its

completion. Also, all aerodynamicists strongly give acceptance to the existence of vortex rings some distance from the plane of the wings. The latter was utilized as a modeling fundamental by [12]. Furthermore, the contraction process requires just one wing span length for its completion, thus this aerodynamic process has more instantaneous influence on the aerodynamics of the animal wing than the role-up phenomenon. Consequently, the contraction phenomenon is taken for modeling consideration in the current theory.

The wake structure is a twisted complicated vortex sheets shed from the trailing edge of the wing in sympathy with changes in bound circulation along the wing span. We assume the aerodynamic interaction of the vortex sheets is such that far downstream they remain undistorted and travel vertically downwards as a rigid set of equally spaced vortex sheets. It is this mutual interaction and self-movement which causes the sheets to move normal to themselves with velocity ω_s . We neglect the twist of the sheets from tip to centre and assume they are infinite in width. These assumptions will allow us to replace the system of a twisted vortex sheets by an infinite series of parallel vortex plates equally spaced, thereby replacing the complex vortex wake structure by a more simplified two-dimensional flow model that can be solved using complex potential methods which satisfy the condition of no flow through the rigid vortex plate surfaces. If the normal spacing of the plates were too small the air between the plates would all be transported downward. Hence, the continuity requirement would be valid to great extent. Therefore, classical aerodynamic techniques can be satisfactorily applied for animal flight analysis for infinitely small vortex sheets spacing. For large normal spacing between the vortex plates, spaces separating the plates allow some of the air to escape upwards round the edges, consequently reducing the downward momentum. This momentum loss is associated with the dominant feature of the unsteady nature of animal flight and normally called the tip loss effect. This phenomenon causes a decrease in the normal velocity between the vortex sheets since some of the flow will rush radially towards the tip, which implies a significant reduction in the lift at the sheet tip. Thus traditional aerodynamic methods are inappropriate for large spacing and a more elaborate modeling is needed. The primary objective of the current study is therefore to put forward an unsteady fluid dynamic model to account for such loss in the total downward momentum, and therefore allows calculation of induced velocity developed at the wing disk.

The main challenge to this model is the aerodynamic problem of finding the flow past a cascade of rectangular vortex plates immersed in a uniform flow. The boundary condition of no flow through the vortex plates completely determines the vortex plate strength, which can be linked to the bound circulation distribution on the wing.

Historically, Prandtl devised a method which simplifies the mathematical difficulties involved in considering the flow around a series of parallel vortex plates. The Prandtl's tip loading approximation theory or so-called the tip loss factor theory has proved to be very successful in describing the flow

around the vortex plates in application to ideal propellers. Therefore, we introduce Prandtl's approximation theory for the flow past the vortex plates. Prandtl suggested that the flow about a helicoidal surface (similar in shape to the vortex sheets generated during flapping flight) can be simplified by taking the flow around a series of rigid parallel equi-spaced plates moving normal to themselves with constant velocity. Prandtl consequently conceived a method which simplifies the mathematical problems involved in describing the flow around the vortex plates.

V. PRANDTL'S TIP LOADING THEORY

The preceding analysis is set to establish a circulation distribution formula across the wing span via Prandtl's tip theory [20]. The aerodynamic problem is to find the flow past a cascade of parallel vortex plates of normal spacing l of length $2R$ in a uniform flow of speed ω_s . These plates apparently have no load on them. At each plate there is a discontinuous change in Φ (velocity potential), due to a discontinuous change in the velocity parallel to the plate. The notations utilized throughout the succeeding derivation are those commonly used in conformal transformation. Circulation is mathematically given by

$$\Gamma = |\Phi - (-\Phi)| = 2|\Phi|. \quad (10)$$

The two-dimensional wake model is graphically shown in Fig. 2., the Z -plane ($z=x+iy$) is used to present the vortex elements.

The conformal transformation is needed to simplify the problem for the physical Z -plane to the ζ -plane ($\zeta=\xi+i\eta$) by taking

$$\zeta = e^{-\frac{\pi z}{l}i} \quad (11)$$

Evidently the flow around the plates is reduced to circulatory flow around a flat plate of length 2 units. If we let

$$\xi = Z + \frac{1}{2Z} \quad (12)$$

Consequently the flat laming is transformed into a circle of radius 1/2 unit and centre at (0,0). Hence if

$$W = \Phi + i\Psi, \quad (13)$$

then the complex potential becomes

$$W = \frac{-i\Gamma_0}{2\pi} \log(2Z), \quad (14)$$

for the circulatory flow around a circle. However, from equation (12)

$$Z = \frac{-\zeta \pm \sqrt{\zeta^2 - 1}}{2}. \quad (15)$$

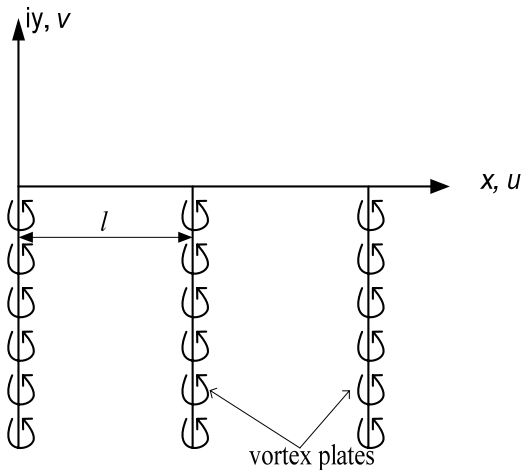


Fig. 2 Circulation distribution along the vortex plates. l is the normal spacing between vortex plates.

Simple algebra easily yields

$$W = \frac{\Gamma_0}{2\pi} \cos^{-1} e^{-i\pi z/l}, \tag{16}$$

where $l (= \hat{T}T\omega_s)$ is the normal spacing of the plates. The obtained function satisfies the condition of no flow through the vortex plates and both velocity components u and v approach zero and ω_s respectively as y approaches infinity. Along $x=0, \Psi=0$, for negative values of y , it gives

$$\Phi = \frac{\Gamma_0}{2\pi} \cos^{-1} e^{\pi y/l}. \tag{17}$$

It is apparent that as $y \rightarrow \infty, \frac{dW}{dZ} = u - iv = \frac{\Gamma_0}{2l} = \omega_s$. The elimination of the infinite velocity at the tip plates demands that we impose a Kutta condition at the tip plates with the requirement $\Phi=0$; this is because there is a pressure equalization from the bottom to the top of the wing; so we take $y = -(R-r)$. The circulation around the plate at distance r is therefore given by

$$\Gamma(r) = \frac{2}{\pi} \omega_s l \cos^{-1} e^{-\frac{\pi}{l}(R-r)}. \tag{18}$$

Prandtl's approximation is assumed to give the variation of the circulation along the wing span of the animal's wing. Thus, we find a value zero at the tip and symmetrical around the centre line of the wing and so the bound circulation distribution along the wing span (so we put $b=R$), after substituting for normal spacing parameter f from equation (3), equation (18) becomes

$$\Gamma(\chi) = \frac{2\pi b^2}{\hat{T}Tf^2} \cos^{-1} e^{-f(1-|\chi|)}, \tag{19}$$

where $\chi = r/b$, which is zero at the wing root and 1 at the wing tip.

VI. MATHEMATICAL FORMULATION

We present the subsequent technique to determine a mean value for the induced velocity generated at the wing disk $\bar{\omega}_d$. This analysis constitutes of a threefold process. First the establishment of a straightforward relationship between f and K and between the wing swept area and initial plate area, and this will yield to the computation of vortex plate dimensions. Second the mathematical presentation of the mean induced velocity in terms of the normal spacing parameter f and stroke angle. Third the determination of mean induced velocity in the vanishing of wake spacing.

A. Determination of vortex plate dimensions

The creation of lift force of a wing is tied to the existing of lifting (bound) vortex within the wing. The bound vorticity, in case of animal hovering flight, consists of two distinguished vortex types: the 'shed vorticity,' which is shed as a result of changes in circulation during the wing beat and the 'trailing vorticity,' which is passed into the wake as a consequence of circulation changing along the wing span; the latter is shed from the trailing edges of the wing to conform to Helmholtz theorem of vortex continuity, or, in other words, formation of a trailing sheet behind the wing is inevitable due to the pressure differences in the spanwise direction as a result of generating lift around the wing. The shed vorticity is of relatively little importance to the aerodynamics of the wing and it would present considerable difficulties to quantify theoretically, and therefore it is recommended that we neglect this type of vorticity in our modeling; other popular theories [12,13] have considered such assumption. In accordance with aerodynamic principles the lift developed by the wing is in a manner that it decreases from a specific value at the wing root to zero at the wing tip. If at a section χ ($0 \leq \chi \leq 1$) from the centre line of the wing the bound circulation is $\Gamma(\chi)$ and in going from χ to $\chi + d\chi$ the bound circulation decreases to $\Gamma(\chi) - d\Gamma(\chi)$, therefore a trailing vorticity of strength $-(d\Gamma/d\chi)d\chi$ must be shed into the wake to conform to Helmholtz theorem of vortex continuity. The total circulation of the bound vortex is therefore given by

$$\Gamma_T = - \int_0^1 (d\Gamma/d\chi) d\chi = \Gamma(\chi = 0). \tag{20}$$

This is equal to the maximum circulation which occurs at the centre line of the wing, so

$$\Gamma_T = \frac{2\pi b^2}{\hat{T}Tf^2} \cos^{-1} e^{-f}. \tag{21}$$

This amount of circulation does not experience any reduction in magnitude once it is deposited in the wake. It is generated in every powered stroke; it is constant everywhere in the flow

field for a given stroke amplitude for a particular animal species even though such vortex plate may undergo some contraction during its journey far downstream providing that it remains stable and does not break away. Contraction apparently redistributes the circulation along the length of the vortex plates and the total circulation remains always constant. There are two aerodynamic principles however governing the bound circulation, one the wing tip loading must be zero, second the total circulation stays constant. In accordance with these two principles, the spanwise distribution of circulation given by equation (19) is considered to give the flow around the vortex plates, and χ can be thought of as a normalizing non-dimensional length which gives values of 0 at the centre line of the plate and 1 at the tip plate.

Vortex sheet is primarily the main physical product of hovering flapping action and the impulse associated with it is important to determine in order to progress in the current modeling. Obviously this sheet undergoes the powerful basic principle of contraction phenomenon once it commences to convect downward away from the tracings of the beating wings. It is well-established that contraction has greater influence on the vortex sheet during its presence in the neighborhood of the bound circulation. The momentum correlated with this vortex sheet is realistically conserved and does not suffer any loss due to the action of the unavoidable process of contraction. The impulse associated with the initial vortex plate acts vertically upward perpendicular to the plane of the planar plate; this impulse is merely responsible for balancing the animal's weight for the duration of $\hat{T}T$. We assume that the total impulse required to generate the vortex plate is not quantitatively influenced whether it is generated in the vicinity of other vortex plates or away from them. The total momentum associated with this vortex plate is given by plate area A_i times total plate circulation Γ_T times fluid density ρ . This impulse holds the animal of weight $M_b g$ airborne at a fixed point in space for the duration $\hat{T}T$. Newton's second law states that the rate change of momentum is equal to the force that is sustaining, therefore

$$\frac{d(\Gamma_T A_i \rho)}{dt} = \frac{\Gamma_T A_i \rho}{\hat{T}T} = M_b g. \quad (22)$$

On substituting for Γ_T from equation (20) into equation (22), so the initial plate area becomes

$$A_i = \frac{\hat{T}^2 T^2 f^2 M_b g}{2\pi \rho b^2 \cos^{-1} e^{-f}}. \quad (23)$$

Divide by $2\Psi_m b^2$ and substitute for K from equation (6), so the ratio of initial plate area to swept area $A_d (= 2\Psi_m b^2)$ is

$$\frac{A_i}{A_d} = \frac{\pi K f^2}{\cos^{-1} e^{-f}}. \quad (24)$$

One particular advantage of this model lies in the fact that Prandtl's approximation theory links remarkably the bound

circulation with the induced velocity far downstream. This property coupled with the hypothetical assumption that the vortex sheet force impulse being equal to the animal's weight can be utilized to combine mathematically the normal spacing parameter f and hovering parameter K in a straightforward fashion. Vorticity is shed from the trailing edge of the wing in the form of a complex vortex sheet. This sheet is a surface of discontinuity and its velocity is the sum of a discontinuous tangential velocity and a continuous normal velocity component. The latter is the velocity with which the vortex sheet is convected in ideal fluid motion; in this model we consider the normal velocity component as the induced velocity far downstream ω_s . Initially, the generated vortex sheet is assumed to lie wholly along the tracings of the beating wings before it starts to convect vertically downwards. An element of width $\partial\chi$ of vortex sheet has strength $-(d\Gamma/d\chi)\partial\chi$. The impulse generated by this element is

$$dI(\chi) = -\rho \frac{d\Gamma}{d\chi} \partial\chi 2b^2 \chi^2 \Psi_m. \quad (25)$$

The total impulse generated can be determined by summing the contributions of all vortex sheet elements shed as a result of the wings beating from $+\Psi_m$ to $-\Psi_m$, so

$$I = -2\rho b^2 \Psi_m \int_0^1 \chi^2 \frac{d\Gamma}{d\chi} d\chi. \quad (26)$$

Integrating by parts gives

$$I = 4\rho b^2 \Psi_m \int_0^1 \chi \Gamma(\chi) d\chi. \quad (27)$$

This impulse must be sufficient to maintain the hovering animal at a fixed point in space for the duration of the wing stroke period $\hat{T}T$. Thus

$$\frac{I}{\hat{T}T} = M_b g. \quad (28)$$

After substitution for $\Gamma(\chi)$ and I , equation (27) becomes

$$\frac{\hat{T}^2 T^2 M_b g}{4\pi^2 \rho b^4 \Psi_m} = \frac{2}{\pi f^2} \int_0^1 \chi \cos^{-1} e^{-f(1-\chi)} d\chi. \quad (29)$$

The left hand-side of equation (29) has already been defined as the hovering parameter K . We define the non-dimensional impulse of the vortex sheet as

$$I_f = 2 \int_0^1 \frac{\chi \Gamma(\chi)}{\Gamma_T} d\chi = 2 \int_0^1 \frac{\chi \cos^{-1} e^{-f(1-\chi)}}{\cos^{-1} e^{-f}} d\chi. \quad (30)$$

Combining equation (29) and equation (30) yields

$$K = \frac{I_f \cos^{-1} e^{-f}}{\pi f^2}. \tag{31}$$

It can be deduced from equations (24) and (31) that

$$\frac{A_i}{A_d} = I_f. \tag{32}$$

Mathematically, I_f slowly approaches its final theoretical limit. This implies that no perfectly horizontal stroke plane is aerodynamically possible because theoretically the final limit of I_f requires a very high value of f to reach and such value is improbable to be obtained from the known hovering animal. Furthermore, whenever any flapping wing is engaged in lift development an additional velocity field is induced at the wing plane in order to accord with aerodynamic principles. This induced velocity automatically establishes an inclination in the stroke plane to allow the earliest part of the vortex sheet generated at the highest point of wing elevation to convect vertically downward, and by the end of the stroke the whole sheet generated will be brought down to a horizontal plane and its associated momentum will therefore be vertical. Ellington (1984) revealed clearly in his filmings that all hovering insects seem to have a noticeably inclined stroke plane angle.

The relationship in equation (32) can be utilized to find the initial vortex plate dimensions of area ($A_i = 2\Psi_m I_f b^2$). If we assume that the contraction phenomenon acts equally along the circumference of the vortex plate, then the length of the plate is taken as $2\sqrt{I_f} b$ and the width as $\Psi_m \sqrt{I_f} b$. This evidently gives a rectangular shape for the initial vortex plate.

B. Determination of mean induced velocity

We have assumed that the rate of change of vertical impulse dI/dt of the vortex sheet is equal to that of the initial horizontal vortex plate, so we can mathematically write

$$\frac{dI}{dt} = 2\rho\omega_d^2 dA_d = 2\rho\omega_i^2 dA_i, \tag{33}$$

where ω_d and ω_i are the local induced velocities along the wing disk and the initial vortex plate respectively. From the relationship between A_d and A_i , equation (33) can be written as

$$\omega_d = \sqrt{I_f} \omega_i. \tag{34}$$

As a result of mutual interaction among the vortex plates, the induced velocity of the initial vortex plate ω_i will increase as the plate travels vertically downwards. The increase in the initial vortex plate velocity can be expressed as

$$\omega_s = \omega_i + 2\omega_a \tag{35}$$

where ω_a is the axial induced velocity component due to a semi-infinite chain of vortex plates and can be accurately calculated by the Biot-Savart Law. Using equation (34) and substituting for ω_i from equation (35) and for ω_s from equation (2) and taking the mean yield

$$\frac{\bar{\omega}_d}{\omega_i} = \frac{\sqrt{I_f}}{f} \int_0^1 \left[1 - 2 \frac{\omega_a(\zeta)}{\omega_s} \right] d\zeta. \tag{36}$$

The purpose of the subsequent material is to present a derivation of expressions for the induced velocity field due to a particular class of vorticity distribution using the Biot-Savart Law. Here, the wake structure is a chain of finite strength, identically similar rectangular planar vortex plates moving vertically downwards with equal speeds. One qualifying aspect of this vortex representation of the wake structure considered here is the practicality in integrating the Biot-Savart law.

Consider the rectangular vortex plate with sides $2\sqrt{I_f} b$ and $\Psi_m \sqrt{I_f} b$. A small vortex filament of length ∂y (see Fig. 3.), strength $(\partial\Gamma/\partial\tau_1) \partial\tau_1$, located at a point $P_1(r_1, y, 0)$ in an idealized incompressible, inviscid potential flow. The velocity induced by this filament at a point $P_2(r_2, 0, z)$ in the field can be calculated with the help of Biot-Savart Law. We start with writing

$$\partial\omega/\partial\tau_1 = \partial\omega/\partial\Gamma \partial\Gamma/\partial\tau_1, \tag{37}$$

where $\partial\omega/\partial\Gamma$ is the velocity per unit circulation induced at P_2 , $\partial\omega/\partial\Gamma$ can be given by the Biot-Savart Law, thus

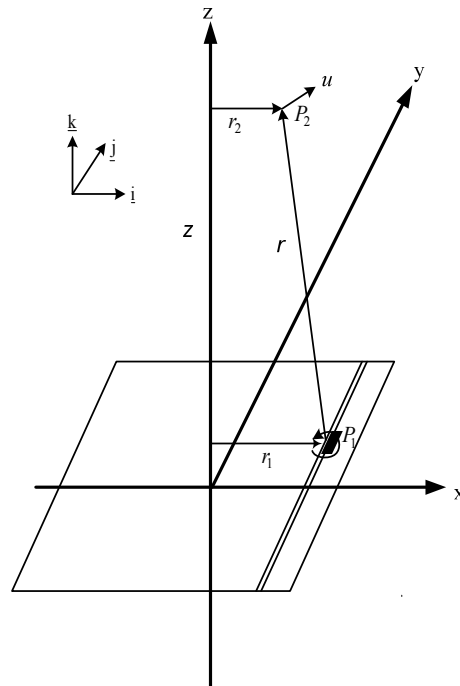


Fig. 3. Notation for calculation of induced velocity field by a

rectangular vortex plate. Point $P_1(r_1, y, 0)$ on the vortex plate where a vortex filament of length ∂y and of strength $(\partial \Gamma / \partial r_1) \partial r_1$ is situated. Field point $P_2(r_2, 0, z)$ where a velocity field u is generated.

$$\partial \omega / \partial \Gamma = -\frac{1}{4\pi} \int \frac{r \times ds}{|r|^3}, \tag{38}$$

where ds is the differential element of the vortex and simply is equal to $dy \underline{j}$ and r is the radius vector from P_1 , where a differential element ds is located to P_2 in the field and written as $r = (r_2 - r_1)\underline{i} + y \underline{j} + z\underline{k}$

$$r = (r_2 - r_1)\underline{i} + y \underline{j} + z\underline{k} \tag{39}$$

Thus $r \times ds = (z\underline{i} - (r_2 - r_1)\underline{k}) dy$.

The velocity components induced at P_2 due to the aerodynamic influence of one neighboring vortex plate therefore are

$$\omega_a = \frac{1}{4\pi} \int_{-b\sqrt{I_f}}^{+b\sqrt{I_f}} \frac{\partial \Gamma}{\partial r_1} dr \int_{-y_1}^{+y_1} \frac{r_2 - r_1}{[(r_2 - r_1)^2 + y^2 + z^2]^{3/2}} dy, \tag{40}$$

where $y_1 = \frac{1}{2} \Psi_m b \sqrt{I_f}$ and ω_a is the axial induced velocity component, and

$$\omega_r = \frac{-1}{4\pi} \int_{-b\sqrt{I_f}}^{+b\sqrt{I_f}} \frac{\partial \Gamma}{\partial r_1} dr_1 \int_{-y_1}^{+y_1} \frac{z}{[(r_2 - r_1)^2 + y^2 + z^2]^{3/2}} dy, \tag{41}$$

where ω_r is the radial induced velocity component. The interior integral for both equations (40) and (41) can be easily solved by making the following substitution, $y = \sqrt{(r_2 - r_1)^2 + z^2} \tan \Theta$ where Θ is a dummy variable, consequently

$$\omega_a = \frac{\Psi_m b \sqrt{I_f}}{4\pi} \int_{-b\sqrt{I_f}}^{+b\sqrt{I_f}} \frac{(r_2 - r_1) \partial \Gamma}{[(r_2 - r_1)^2 + \frac{1}{4} \Psi_m^2 b^2 I_f + z^2]^{1/2} [(r_2 - r_1)^2 + z^2]} dr_1, \tag{42}$$

and

$$\omega_r = \frac{-\Psi_m b \sqrt{I_f}}{4\pi} \int_{-b\sqrt{I_f}}^{+b\sqrt{I_f}} \frac{z \partial \Gamma}{[(r_2 - r_1)^2 + \frac{1}{4} \Psi_m^2 b^2 I_f + z^2]^{1/2} [(r_2 - r_1)^2 + z^2]} dr_1. \tag{43}$$

To simplify these equations we write $\zeta = r_2 / b \sqrt{I_f}$, $\chi = r_1 / b \sqrt{I_f}$, therefore equations (42) and (43) become

$$\omega_a(\zeta) = \frac{\Psi_m}{4\pi b \sqrt{I_f}} \int_{-1}^1 \frac{(\zeta - \chi) \partial \Gamma}{[(\zeta - \chi)^2 + \bar{B}^2]^{1/2} [(\zeta - \chi)^2 + \bar{A}^2]} d\chi, \tag{44}$$

and

$$\omega_r(\zeta) = \frac{-\Psi_m}{4\pi b \sqrt{I_f}} \int_{-1}^1 \frac{\tilde{z} \partial \Gamma}{[(\zeta - \chi)^2 + \bar{B}^2]^{1/2} [(\zeta - \chi)^2 + \bar{A}^2]} d\chi, \tag{45}$$

where $\bar{A} = \frac{\pi}{f \sqrt{I_f}}$ and $\bar{B} = \sqrt{\left[\left(\frac{\pi}{f \sqrt{I_f}} \right)^2 + \left(\frac{\Psi_m}{2} \right)^2 \right]}$.

Integrating by parts with respect to χ , substituting for the radial circulation distribution $\Gamma(\chi)$ of the vortex plate, and summing the contributions of the semi-infinite chain of vortex plates give

$$\frac{\omega_a(\zeta)}{\omega_s} = \frac{\Psi_m}{2\pi f \sqrt{I_f}} \sum_{N=1}^{\infty} \int_{-1}^1 \frac{\cos^{-1} e^{-f(1-|\chi|)} [-2(\zeta - \chi)^4 - \bar{B}_N^2 (\zeta - \chi)^2 + \bar{B}_N^2 \bar{A}_N^2]}{[(\zeta - \chi)^2 + \bar{B}_N^2]^{3/2} [(\zeta - \chi)^2 + \bar{A}_N^2]^2} d\chi, \tag{46}$$

$$\frac{\omega_r(\zeta)}{\omega_s} = \frac{-\Psi_m}{2\pi f \sqrt{I_f}} \sum_{N=1}^{\infty} \bar{A}_N \int_{-1}^1 \frac{\cos^{-1} e^{-f(1-|\chi|)} [(\zeta - \chi)(3(\zeta - \chi)^2 + 2\bar{B}_N^2 + \bar{A}_N^2)]}{[(\zeta - \chi)^2 + \bar{B}_N^2]^{3/2} [(\zeta - \chi)^2 + \bar{A}_N^2]^2} d\chi, \tag{47}$$

where $\bar{A}_N = \frac{N\pi}{f \sqrt{I_f}}$ and $\bar{B}_N = \sqrt{\left[\left(\frac{N\pi}{f \sqrt{I_f}} \right)^2 + \left(\frac{\Psi_m}{2} \right)^2 \right]}$. The

velocity field u can be expressed as

$$u = \omega_r \underline{i} + \omega_a \underline{k} \tag{48}$$

Equation (46) can be used together with equation (36) to determine straightforwardly the mean induced velocity at the wing disk, $\bar{\omega}_d$, for a given normal spacing parameter f and wing stroke amplitude.

C. Determination of mean induced velocity in the vanishing wake spacing

In the limit of vanishing periodicity ($f \rightarrow \infty$) we anticipate that the circulation is constant along the wing span, and

mathematically $\cos^{-1} e^{-f(1-|\chi|)} \rightarrow \pi/2$ and $I_f \rightarrow 1$.
Therefore equation (47) is reduced to

$$\frac{\omega_a(\zeta)}{\omega_s} = \frac{\Psi_m}{4\pi} \sum_{N=1}^{\infty} \frac{\bar{A}_N}{N} \int_{-1}^1 \frac{-2(\zeta-\chi)^4 - \bar{B}_N^2(\zeta-\chi)^2 + \bar{B}_N^2 \bar{A}_N^2}{[(\zeta-\chi)^2 + \bar{B}_N^2]^{3/2} [(\zeta-\chi)^2 + \bar{A}_N^2]^2} d\chi. \quad (49)$$

We start with $\zeta - \chi = \bar{A}_N \tan \Theta$ so equation (49) becomes

$$\frac{\omega_a(\zeta)}{\omega_s} = \frac{\Psi_m}{4\pi} \sum_{N=1}^{\infty} \frac{1}{N\bar{B}_N} \int_{\Theta_2}^{\Theta_1} \frac{-2k^2 \cos^5 \Theta + (1-4k_1^2)\cos^3 \Theta + 2k_1^2 \cos \Theta}{\nabla^3} d\Theta, \quad (50)$$

where

$$\left. \begin{aligned} \Theta_1 &= \tan^{-1}[(\zeta-1)/\bar{A}_N], \\ \Theta_2 &= \tan^{-1}[(\zeta+1)/\bar{A}_N], \\ \nabla &= \sqrt{1-k^2 \sin^2 \Theta}, \\ k &= \frac{\Psi_m/2}{\bar{B}_N}, \text{ and} \\ k_1 &= \sqrt{1-k^2}. \end{aligned} \right\}$$

From tables of integrals [21], equation (50) can be solved to give

$$\frac{\omega_a(\zeta)}{\omega_s} = -\frac{\Psi_m}{4\pi} \sum_{N=1}^{\infty} \frac{1}{N\bar{B}_N} \left[\frac{\cos^2 \Theta \sin \Theta}{\nabla} \right]_{\Theta_2}^{\Theta_1}. \quad (51)$$

After further simplifications equation (51) becomes

$$\frac{\omega_a(\zeta)}{\omega_s} = \frac{\Psi_m}{4f} \sum_{N=1}^{\infty} \left\{ \frac{(\zeta+1)}{[\bar{A}_N^2 + (\zeta+1)^2] \sqrt{\bar{B}_N^2 + (\zeta+1)^2}} - \frac{(\zeta-1)}{[\bar{A}_N^2 + (\zeta-1)^2] \sqrt{\bar{B}_N^2 + (\zeta-1)^2}} \right\}. \quad (52)$$

This equation does not converge quickly for high values of f , therefore there is a need to eliminate the sum sign in the equation (52). To do so, we will utilize the following mathematical technique which can be represented as follows:

$$\lim_{f \rightarrow \infty} \frac{1}{f} \sum_{N=1}^{\infty} f(N/f) = \int_0^1 f(\xi) d\xi, \quad (53)$$

where $\xi=N/f$. If we let $\xi=N/f$ and $\Psi_m = \pi/2$, and in the vanishing wake spacing ($f \rightarrow \infty$) equation (52) may be written as

$$\frac{\omega_a(\zeta)}{\omega_s} = \frac{\pi}{8} \int_0^1 \left\{ \frac{(\zeta+1)}{[\pi^2 \xi^2 + (\zeta+1)^2] \sqrt{\pi^2 \xi^2 + \frac{\pi^2}{16} + (\zeta+1)^2}} - \frac{(\zeta-1)}{[\pi^2 \xi^2 + (\zeta-1)^2] \sqrt{\pi^2 \xi^2 + \frac{\pi^2}{16} + (\zeta-1)^2}} \right\} d\xi. \quad (54)$$

The integral in equation (54) can be readily solved to produce

$$\frac{\omega_a(\zeta)}{\omega_s} = \frac{1}{2\pi} \left\{ \tan^{-1} \left[\frac{\pi^2/4}{(\zeta+1)\sqrt{(17\pi^2/16) + (\zeta+1)^2}} \right] - \tan^{-1} \left[\frac{\pi^2/4}{(\zeta-1)\sqrt{(17\pi^2/16) + (\zeta-1)^2}} \right] \right\}. \quad (55)$$

In the limit of vanishing wake spacing equation (36) can be written as

$$\frac{\bar{\omega}_d}{\omega_s} = \int_0^1 \left[1 - 2 \frac{\omega_a(\zeta)}{\omega_s} \right] d\zeta. \quad (56)$$

On substitution of equation (55) into equation (56) and solving numerically we obtain $\bar{\omega}_d/\omega_s \approx 0.53$. This is close to the theoretical limit of 0.5.

VII. RESULTS

An overwhelming majority of theoretical studies in animal flight mechanics have primarily concentrated upon determination of energy consumption during hovering and steady forward flights because the energetic cost of flapping flight dictates the life style of living animals. The vortex plate theory presented here is concerned with evaluation of the induced power requirement for animals hovering with horizontal stroke plane angle flight mode ($\hat{T}=1/2$) and inclined stroke plane angle flight mode ($\hat{T}=1$). The current theory recognizes that precise estimate of the induced power requirement during hovering flight phenomenon is a formidable task because no flight theory that can explicitly account for all parameters associated with energy consumption during hovering flight. Any such attempt will doom to failure since our state of knowledge in this regard does not serve us to comprehend categorically the methods of working which employed by flapping wings during their operation and how efficient mechanical power delivered by the muscles of the wings is converted to useful mechanical work. Admittedly, there are many gray areas in such regard that yet to be resolved, therefore any suggested theoretical flight model can not be tested and verified appropriately.

The portion of the mechanical power that is delivered to the environment by the flapping wings in order to support the

body weight during hovering flight is termed as the induced power, and the current flight theory is intended to calculate the induced power. It is also equivalent to the power dissipated in generation the vortex wake system. The mean induced power is calculated as the force supported by both wings ($M_b g$) times the mean induced velocity ($\bar{\omega}_d$). The ratio of the mean induced velocity to wing tip velocity ($\bar{\omega}_d/\omega_t$) is calculated numerically by equation (36) and equation (46). The value of $\bar{\omega}_d/\omega_t$ can be approximated,

TABLE I
MORPHOLOGIC AND KINEMATIC PARAMETERS FOR REPRESENTATIVE HOVERING ANIMALS

Species	Body Mass, M_b (kg)	Semi-span, b (m)	Period, T (s)	Half stroke angle, Ψ_m (deg.)	Hovering parameter, K	Ref.
Horizontal Stroke Plane						
Hummingbird, <i>Amazilia fimbriata</i>	5.1×10^{-3}	0.059	0.0286	60	0.0167	[10]
Crane fly, <i>Tipula obsoleta</i>	0.114×10^{-3}	0.0127	0.022	61	0.0098	[13]
Crane fly, <i>Tipula paludosa</i>	0.498×10^{-3}	0.0174	0.0172	60	0.0078	[13]
Lady bird, <i>Coccinella 7-punctata</i>	0.344×10^{-3}	0.0173	0.0186	88.5	0.0251	[22]
Bumble bee, <i>Bombus lucorum</i>	0.231×10^{-3}	0.0141	0.0072	65	0.0133	[22]
Inclined Stroke Plane						
Pied flycatcher, <i>Ficedula hypoleuca</i>	12×10^{-3}	0.115	0.07	50	0.07815	[23]
Pigeon, <i>Columba livia</i>	333×10^{-3}	0.316	0.15	60	0.1456	[24], [25]
Nectar-feeding bat, <i>Glossophaga soricina</i>	10.5×10^{-3}	0.129	0.0658	60	0.0331	[26]

with an accuracy of $\pm 1\%$, according to the following formula,

$$\frac{\bar{\omega}_d}{\omega_t} = \frac{0.75}{f \cdot 0.9 + 2\lambda/13}, \quad (57)$$

where $\lambda = 2\Psi_m/\pi$. This formula allows a quick estimate of the mean induced velocity for hovering animals provided that f lies between 1 to 12. Indeed, most hovering animals are characterized by normal spacing parameter that lies within this range. For a given hovering parameter K the normal spacing parameter f can be calculated by the following approximated formula

$$f = 42.2337(1 - 1.003 e^{-F(K)}), \quad (58)$$

where $F(K) = 0.01027 K^{-0.6023}$, its accuracy lies within $\pm 1\%$ for all animals.

The theory is applied on a selected number of hovering animals (Table I) and mean induced power is calculated for

each species (see Table II). Rayner's theory (1979) finds that flycatcher needs 0.230 W to hover continuously. However, the current theory gives slightly higher value 0.238 W ($P_i^* \approx 2.03 \text{ W/N}$) and the difference between the two estimated values is about 4%. Full agreement is found for the mean specific induced power requirement for the pigeon between the current theory and that of Rayner's ($P_i^* \approx 3.8 \text{ W/N}$). An extensive calculations for many species have been conducted by the current theory and that of Rayner's and it is found that the two theories give very close estimates for the mean induced power for values of half-stroke angles between 45° and 75° for small hovering animals ($f > 1$). However, the difference becomes greater for high and low values of stroke angles. In fact, the current theory gives lower estimate of mean induced power for low values of half-stroke angles ($< 30^\circ$) than Rayner's theory, and for high values of half-stroke angles ($> 75^\circ$) the current theory gives slightly higher values of mean induced power than Rayner's theory. [26] carried out a study to calculate empirically the cost of hovering for nectar-feeding bat, *Glossophaga soricina* by using a method that based on aerodynamic theory. Their estimates for the mean specific induced power needed for the bat to hover continuously is 1.427W/N, the current theory gives 1.415W/N. Apparently, the agreement is within 1% between the two estimates.

TABLE II
MEAN SPECIFIC INDUCED POWER IN HOVERING

Species	Hovering spacing parameter, f	Wing tip velocity, ω_t (m/s)	Ideal velocity, ω_j (m/s)	Mean specific induced power $P_i^* (= \bar{\omega}_d)$ (W/N or m/s)
Horizontal Stroke Plane				
Hummingbird, <i>Amazilia fimbriata</i>	4.797	12.962	1.674	2.004
Crane fly, <i>Tipula obsoleta</i>	6.452	3.630	0.360	0.418
Crane fly, <i>Tipula paludosa</i>	7.133	6.340	0.560	0.664
Lady bird, <i>Coccinella 7-punctata</i>	3.795	3.790	0.600	0.693
Bumble bee, <i>Bombus lucorum</i>	5.440	12.400	1.430	1.669
Inclined Stroke Plane				
Pied flycatcher, <i>Ficedula hypoleuca</i>	1.932	5.161	1.440	2.026
Pigeon, <i>Columba livia</i>	1.311	6.612	2.520	3.799
Nectar-feeding bat, <i>Glossophaga soricina</i>	3.232	6.160	1.098	1.415

[13] estimated the mean induced power requirements for a wide range of species. The current theory is in a good agreement with Ellington's work. Full agreement has been found for the crane fly, *Tipula obsoleta* and the ladybird, *Coccinella 7-punctata*. Ellington's mean induced power

estimate for the bumble bee is $1.65W/N$ and the current theory gives a value higher by 1% than Ellington's estimate. However, extensive calculations have been conducted on various type of insect species and the agreement between both theories have been found to fall within full agreement and 5% for horizontal stroke plane flight mode.

VIII. CONCLUSION

The current theory calculates the mean induced power requirement during animal hovering flight. The distinguishing characteristics of the current work can be summarized as follows: (1) The current work recognizes that unsteady effects is an important aerodynamical feature with respect to animal flight, (2) the circulation distribution along the vortex plate is calculated via Prandtl's tip theory, unlike previous theories which assume preset circulation distribution profiles, (3) less dramatic assumptions are used in developing the current theory, (4) the simplicity of the vortex structure proposed by the current theory has made modeling mathematically manageable, and (5) the theory is equally applicable to both birds and insects.

A model of a chain of rectangle vortex plates structure is found reasonably appropriate for hovering animals flight phenomenon. This structure has allowed to derive a simple formula for calculation of mean induced power; it is based only on normal spacing parameter f and stroke angle. The current theory anticipates higher values for the mean induced power than traditional approaches which have been found to underestimate the induced power computations.

A comparison with previous theories have been made, a remarkable agreement has been observed with Rayner's theory for inclined stroke plane angle flight mode and Ellington's theory for horizontal stroke plane flight mode, although both theories have different theoretical manifestations of the problem domain from the current theory.

REFERENCES

- [1] C. Van Den Berg, and C. P. Ellington, "The vortex wake of a hovering model hawkmoth," *Philos. Trans. R. Soc. London B*, vol. 352, pp. 317–328, 1997.
- [2] M. H. Dickinson, F. O. Lehmann, and S. P. SANE, "Wing rotation and the aerodynamic basis of insect flight," *Science*, vol. 284, pp. 1954–1960, 1999.
- [3] S. P. Sane and M. H. Dickinson, "The control of flight force by a flapping wing: lift and drag production," *J. Exp. Biol.*, vol. 204, pp. 2607–2626, 2001.
- [4] S. P. Sane and M. H. Dickinson, "The aerodynamic effects of wing rotation and a revised quasi-steady model of flapping flight," *J. Exp. Biol.*, vol. 205, pp. 1087–1096, 2002.
- [5] G. R. Spedding, M. Rosén, and A. Hedenström, "A family of vortex wakes generated by a thrush nightingale in free flight in a wind tunnel over its entire natural range of flight speeds," *J. Exp. Biol.*, vol. 206, pp. 2313–2344, 2003.
- [6] M. F. M. Osborne, "Aerodynamics of flapping flight with application to insects," *J. Exp. Biol.*, vol. 28, pp. 221–245, 1951.
- [7] C. J. Pennycuik, "A wind-tunnel study of gliding flight in the pigeon *Columba livia*," *J. Exp. Biol.*, vol. 49, pp. 509–526, 1968.
- [8] C. J. Pennycuik, *Mechanics of flight In Avian Biology*. Vol. 5 (ed. D. S. Farner and J. R. King), pp. 1–75. New York: Academic Press, 1975.
- [9] T. Weis-Fogh, "Energetics of hovering flight in hummingbirds and in *Drosophila*," *J. Exp. Biol.*, vol. 56, pp. 79–104, 1972.

- [10] T. Weis-Fogh, "Quick estimates of flight fitness in hovering animals, including novel mechanisms for lift production," *J. Exp. Biol.*, vol. 59, pp. 169–230, 1973.
- [11] C. D. Cone, "The aerodynamics of flapping bird flight," *Spec. Sci. Rep. Va Inst. Mar. Sci.*, vol. 52, 1968.
- [12] J. M. V. Rayner, "Vortex theory of animal flight I. vortex wake of a hovering animal," *J. Fluid Mech.*, vol. 91, pp. 697–730, 1979.
- [13] C. P. Ellington, "The aerodynamics of hovering insect flight," *Philos. Trans. R. Soc. London B*, vol. 305, pp. 1–181, 1984.
- [14] S. P. Sane, "Induced airflow in flying insects. I. A theoretical model of the induced flow," *J. Exp. Biol.*, vol. 209, pp. 32–42, 2006.
- [15] L. M. Milne-Thompson, *Theoretical Aerodynamics*. Dover, New York, 1958.
- [16] C. P. Ellington, "The aerodynamics of normal hovering flight," *In Comparative Physiology -Water, Ions and Fluid Mechanics* (ed. K. Schmidt-Nielsen, L. Bolis and S. H. P. Maddrell), Cambridge University Press, pp. 327–345, 1978.
- [17] M. J. Lighthill, "On the Weis-Fogh mechanism of lift generation," *J. Fluid Mech.*, vol. 60, pp. 1–17, 1973.
- [18] T. Weis-Fogh and R. McN. Alexander, "The sustained power output from striated muscle," *In Scale Effects in Animal Locomotion* (ed. T. J. Pedley), London: Academic Press, pp. 511–525, 1977.
- [19] C. J. Pennycuik and M. A. Rezende, "The specific power output of aerobic muscle, related to the power density of mitochondria," *J. Exp. Biol.*, vol. 108, pp. 377–392, 1984.
- [20] A. Betz and L. Prandtl, *Schraubenpropeller mit geringstem Energieverlust*. Nachr. Ges. Wiss. Göttingen, pp. 193–213, 1919.
- [21] I. S. Gradshteyn and I. M. Ryzhik, *Tables of Integrals, Series and Products*. Academic Press, New York, section 2.58, 1965.
- [22] O. Sotavalta, "The essential factor regulating the wing stroke frequency of insects in wing mutilation and loading experiments at subatmospheric," *Ann. Zool. Soc.*, vol. 15 (2), pp. 1–67, 1952.

Dr. Khaled M. S. Faqih received B.Sc. (Hons.) in aeronautical and astronautical engineering degree from the University of Southampton, England, in 1983. He joined the Royal Jordanian Air Force for 16 years. He received a master degree in Information Technology from the University of Science Malaysia, Malaysia, in 2002. He has been working as a lecturer since 2002 at Al al-Bayt University, Jordan (Information Technology faculty), teaching various topics in information technology. He received a PhD in Management Information Systems, in 2010, from the University of Banking and Financial Sciences, Jordan. His research interests, in addition to the aerodynamics of natural flight, include web usability, web computing and online and mobile shopping adoption modeling.